Journal of Structural Geology, Vol. 14, No. 10, pp. 1149 to 1156, 1992
Printed in Great Britain

0191-8141/92 $05.00 + 0.00

Displacement–length scaling relationship for faults: data synthesis and discussion

PATIENCE A. COWIE* and CHRISTOPHER H. SCHOLZ

Lamont–Doherty Geological Observatory and Department of Geological Sciences, Columbia University, Palisades, NY 10964-0190, U.S.A.

(*Received* 23 *August* 1991; *accepted in revised form* 27 *April* 1992)

Abstract—It is observed that the amount of displacement (d) on a fault is proportional to the mapped trace length L. The exact form of the fault scaling relationship, i.e. $d = f(L)$, is still a subject of some disagreement. A number of workers have interpreted data from individual data sets as indicating a linear relationship between d and L. However, these individual data sets have large scatter and a limited range of scale, so their interpretations are not fully conclusive. Other workers have interpreted combinations of different data sets, taken together, and concluded that the d vs L scaling relationship is non-linear. Fault growth models, however, indicate that the scaling relationship should depend on rock properties so correlations using combined data sets may be questionable.

This paper presents a synthesis of published data sets on the displacements and lengths of faults. A summary of each data set is given, including: the geologic setting; the mode of faulting (normal/thrust/strike-slip); and the measurement methods used to obtain the displacement and length data. Sources of scatter in the data due to geologic effects and measurement procedures are reviewed. Our preferred interpretation is that the d–L relationship is linear with a possible cross-over phenomenon between small and large faults, but the unambiguous resolution of this question will require some significant improvements in the existing database.

INTRODUCTION

FIELD observations indicate that there is a correlation between the maximum amount of displacement on a fault (d) and the length of the fault trace (L). For example, faults of tens of kilometers in length typically have displacements of the order of hundreds of meters, while faults of a few meters in length have offsets of the order of only a few centimeters. This observed correlation refers to *bounded* faults, i.e. faults of finite length that are not plate boundaries and do not terminate in a plate boundary. Examples of unbounded faults are the San Andreas fault in California, the Alpine fault in New Zealand, and also oceanic transform faults; the displacements and lengths of these faults are controlled by plate kinematics and geometry. Otherwise most continental and oceanic faults associated with plate boundaries and in interplate regions are bounded. The characteristic of a bounded fault is that the displacement decreases to zero at the fault tips. If, as is often the case, several faults are structurally linked together, the composite structure, or fault zone, is also typically bounded since the displacement can be observed to go to zero at the ends of the fault zone. A correlation between d and L is only to be expected for bounded faults because the accumulation of displacement on such a fault will increase the strain concentration at the fault tips, thus causing it to grow in length.

There are several reasons why establishing the form of the fault scaling relationship is useful. Since the basic principles were set out by Anderson in 1942, field geologists have been particularly interested in faulting as a geometrical problem: for example, piggy-back thrusting (Boyer & Elliott 1982); or domino and listric styles of normal faulting (e.g. Wernicke & Burchfiel 1982, Gibbs 1984). These idealizations of fault geometry are usually restricted to a two-dimensional view, e.g. a cross-section, which requires specification of the displacement on a fault but not its length. An important consequence of a displacement–length relationship therefore, is that it provides a basis for extrapolating a two-dimensional view of faults into the third dimension. Furthermore, the relationship between displacement on a fault and its length implies a description of fault growth over geologic time. That is, as a fault gradually accumulates displacement the dimensions of the fault surface must also increase to maintain the scaling relationship (Walsh & Watterson 1988, Cowie & Scholz 1992a). Furthermore, Scholz & Cowie (1990) showed that if a relationship between d and L can be established for a population of faults in a deformed region, the total brittle strain can be calculated when only the length, or the displacement, distribution of the faults is known. In another application, Gibson *et al.* (1989) and Schlische (1991) have used displacement–length relationships to model the three-dimensional stratigraphic development of fault controlled sedimentary basins.

Data relevant to the scaling of d with L have been collected for the various fault types (normal/thrust/strike-slip), in a wide variety of tectonic environments, and for a range of length scales. Individual data sets are usually restricted to a single rock type and either a single tectonic environment or length scale. Some workers

*Present address: Laboratoire de Physique de la Matière Condensée, Université de Nice—Sophia Antipolis, CNRS URA 190, Parc Valrose, Nice 06000, France.

have interpreted their individual data set as being most consistent with a linear relationship (e.g. Elliot 1976, Ranalli 1977, Muraoka & Kamata 1983, Opheim & Gudmundsson 1989. Villemin *et al.* in press). On the other hand, other workers who have combined a number of individual data sets have reached very different conclusions. Watterson (1986) and Walsh & Watterson (1988), studying a combined data set that included Elliot's (1976) data and Muraoka & Kamata's (1983) data along with their own data, primarily from British coalfields, interpreted it to mean that $d \propto L^2$. Using a different group of data sets, Marrett & Allmendinger (1991) made a least-squares best fit to the data and concluded that $d \propto L^{1.5}$. These two interpretations differ in more than just the value of the exponent. Walsh & Watterson (1988) made their interpretation by way of a fault growth model originally proposed by Watterson (1986), in which

$$d = \frac{L^2}{P}, \tag{1}$$

where P is a variable related to rock properties. Since P can be expected to vary with rock type and tectonic environment and perhaps fault type as well, Walsh & Watterson (1988) argued with regard to their own analysis that: "The best-fit line (on a log–log plot) has a slope of 1.58 but . . . the data will not ideally lie along a single line and a regression line has little significance". Consequently, they assumed an exponent of 2 in that paper. More recently, however, Walsh & Watterson (1991) have accepted the exponent of 1.5 that Marrett & Allmendinger (1991) obtained, although they did not state why they now consider the regression line to be significant.

We have recently presented a model of fault growth based on a post-yield fracture mechanics description of a fault (Cowie & Scholz 1992b). This model predicts that a fault loaded by a uniform (time averaged) remote stress grows in a self-similar manner such that:

$$d = \frac{C(\sigma_o - \sigma_f)L}{\mu}, \tag{2}$$

where σ_o is the shear strength of the surrounding rock, μ is its shear modulus, σ_f is the frictional shear stress on the fault, and C is a constant that depends on the ratio of the remote stress loading the fault to the rock shear strength. This model predicts linear scaling between d and L but the constant of proportionality will vary with rock type and tectonic environment. Thus, according to this model individual data sets should not be interpreted collectively. In the same paper, we stated that the predictions of our model are consistent with the available data for faults, but space did not permit a detailed discussion of this point. In the light of the various conflicting interpretations of these fault data, as outlined above, we discuss the data in detail here in order to show how we can support our interpretation, and in what manner we differ from the interpretation of others.

AREAS OF STUDY AND MEASUREMENT PROCEDURES

Western Canada

Elliott (1976) was the first geologist to publish a correlation between the displacement and length of faults. He studied Cretaceous–Tertiary thrust faults in the Canadian Rockies that deform Paleozoic rocks and the syn-orogenic foreland basin deposits. The displacement measurements were obtained from restored cross-sections. The displacement measurements thus correspond to the separation of a particular stratigraphic unit. Only the maximum displacement on each thrust fault was estimated. The length measurements were obtained from fault trace mapping. Elliott (1976) published data for 20 thrusts shown as a graph (Elliott's fig. 3) but not tabulated. This data set was subsequently revised and augmented to give a total of 29 data points shown in Fig. 1(a). Unfortunately these revised data were only presented as part of a seminar for the Canadian Society of Petroleum Geologists (Elliott unpublished manuscript). The faults range in length from tens to hundreds of kilometers. Elliott (1976) did not discuss the details of the measurement methods nor the magnitude of the errors associated with each data point.

Western U.S.A.

Krantz (1988) conducted a detailed study of the geometry and displacements of more than 30 normal faults within an area of 25 km^2 at Chimney Rock in the northern San Rafael Swell of central Utah. Figure 1(b) shows displacement and length measurements for the 16 largest faults in that area. The faults in this study range in length from a few hundreds of meters to several kilometers and offset Jurassic age Navajo Sandstone and the overlying Carmel Formation. Many of the faults can be traced for their entire length along strike so that both terminations of the fault are seen. The largest fault in the population is approximately 5 km long and has an offset of about 30 m. The structures are well exposed at Chimney Rock and displacement measurements were made at approximately 100 m spacing along the fault traces.

United Kingdom

Walsh & Watterson (1987) present an analysis of the displacement distributions on normal faults in the East Pennine coalfieds of England. The faults cut Carboniferous Coal Measure rocks that consist of repeated sequences of sandstone, limestone and shale with coal horizons. The data were obtained from mine plans some of which were published by Rippon (1985). Walsh & Watterson (1987) present data from 25 individual faults. Most of the data were obtained from diagrams of contoured fault displacement. Their table 1 shows interpolated displacement measurements along radii or chords parallel to the strike of the fault from the middle of the

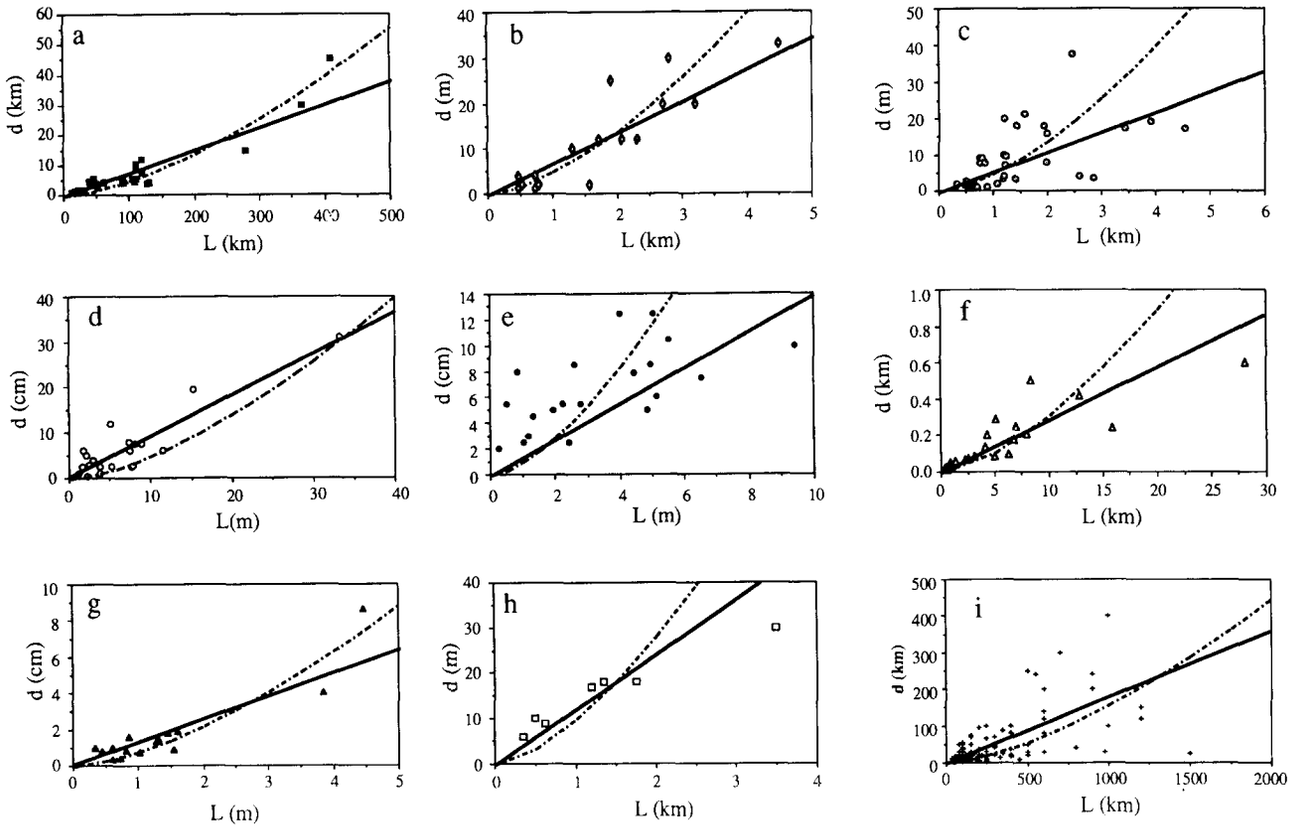

Fig. 1. Plots of maximum fault displacement vs fault length for nine different data sets: (a) Elliott (1976); (b) Krantz (1988); (c) Walsh & Watterson (1987); (d) Peacock & Sanderson (1991); (e) Peacock (1991); (f) Villemin *et al.* (in press); (g) Muraoka & Kamata (1983); (h) Opheim & Gudmundsson (1989); (i) MacMillan (1975).

fault out to the tip. A total of 34 radial profiles are given, i.e. some faults are sampled along their entire length giving two radial profiles. These workers document carefully the quality controls applied to these fault data, in particular the maximum displacement is clearly identifiable in each case and there is no intersection with other faults or obvious interference from adjacent faults. For the purposes of comparison with the other data sets these data are plotted in Fig. 1(c) assuming that the length of the fault is equal to twice the radius. This is a reasonable assumption because in most cases the maximum fault displacement occurs approximately in the center of the fault (Walsh & Watterson 1987, 1988). Fault lengths in this data set range from several hundred meters to a few kilometers. Sources of measurement error are fully discussed. In addition to their tabulated data, Walsh & Watterson (1988) also show a larger untabulated data set that plots as an almost equant scatter field on their log–log plot. For these reasons, we do not attempt to find an individual correlation for this data set, although we later include it in a log–log plot along with the other data sets (see Fig. 3).

Peacock & Sanderson (1991) measured detailed displacement profiles along a normal fault zone, approximately 80 m long, exposed on a wave cut platform on the Somerset coastline at Kilve. A total of 20 displacement–length measurements were obtained from individual fault segments that varied in length from a few meters to about 30 m (Fig. 1d). The faults are exposed in Lower Jurassic limestone and faulting is thought to be related to opening of the Bristol Channel in the Jurassic. Peacock & Sanderson (1991) also constructed detailed displacement profiles along the fault traces. The individual segments interact to varying degrees. The effect of interaction is shown by the asymmetry in the displacement profiles, i.e. the maximum displacement is usually offset from the center of the trace. Displacement gradients towards the tips of interacting segments are generally steeper, suggesting that the segments are shorter than they would be if they were isolated faults. The d–L ratio for the whole fault zone is 3.6×10^{-3} as compared to an average d–L ratio for the segments of 7.6×10^{-3}. The size of this effect, therefore, is about a factor of 2.

Peacock (1991) presents a study of strike-slip faults near Kircudbright, Scotland. Two outcrops have been mapped in detail at Raeberry and Gypsy Point where faults, with length of less than 10 m, are exposed in Silurian greywackes and sandstones. The faulting is believed to be Caledonian in age. Displacement–length measurements were obtained for 20 faults (Fig. 1e). Detailed displacement profiles along fault traces. i.e. parallel to the slip vector, are also presented. The measurement methods are well documented. As in the Peacock & Sanderson (1991) study, these faults are made up of segments that are probably interacting, and also, as they strike across bedding, they show the effects of varying rock type on fault growth and termination.

Walsh (personal communication) suggested that the effects of fault interaction and lithologic variation in the Peacock & Sanderson (1991) and the Peacock (1991)

data sets may preclude a meaningful analysis of the displacement–length relationship. However, since both studies consist of careful and well-documented measurements, we see no reason to exclude these data from our analysis *a priori*, and furthermore, they provide data in a scale range not well sampled by others.

France

Villemin *et al.* (in press) used structural information from mine plans to analyse the displacement distributions on normal faults in the Lorraine coal field, NE France. The faults cut Carboniferous to early Permian coal measure deposits. The faulting appears to be both syn-depositional (early Permian) and post-depositional. Preliminary work (Villemin & Sunwoo 1987) showed an analysis of the spatial distribution of these faults. A log–log plot of fault displacement vs fault length for more than 100 faults was also presented in that manuscript but these data show a lot of variability. After applying quality controls to these data, similar to those of Walsh & Watterson (1987, 1988) described above, Villemin *et al.* (in press) presented a culled data set of 26 faults shown in Fig. 1(f). The measurement methods and the sources of measurement error are well documented in Villemin *et al.* (in press). The faults in this data set range in length from about 1 km to a few tens of kilometers.

Japan

Muraoka & Kamata (1983) measured displacement profiles for a set of normal faults exposed in Pleistocene lake sediments of the Kusu Group. These sedimentary rocks are exposed on the north flank of Kuju volcano in Kyushu, Japan. The faults are Quaternary in age, have lengths up to 1 m or so, and are related to volcanic activity. Bedding planes are nearly horizontal and are cut by fault surfaces at an angle of up to 80°. The trace lengths of 15 faults were measured in cliff sections and detailed displacement profiles were constructed parallel to the slip vector, i.e. down-dip, by matching the sedimentary horizons across the faults. These data are shown in Fig. 1(g). Muraoka & Kamata (1983) present a full discussion of their measurement methods.

Iceland

Opheim & Gudmundsson (1989) measured profiles along seven normal faults, of up to a few kilometers in length, in the Krafla fissure swarm in the northern part of the rift zone (Fig. 1h). These faults formed in Holocene (post-glacial) flood basalt flows. Many of these normal faults are gaping at the surface reflecting that they develop from sets of tension fractures (Gudmundsson 1987a). Opheim & Gudmundsson (1989) measured vertical fault throw and opening profiles at points spaced 25–50 m apart along these faults. Trace lengths were measured from aerial photographs. The measurement methods are well documented. The main source of error in these data is that in some cases the amount of opening is overestimated when the sides of the fractures have collapsed. Gudmundsson (1987a,b) mapped faults in the Vogar and Thingvellir fissure swarms in southwestern, Iceland. Gudmundsson (in press) calculated a linear regression between fault throw and length for fractures in these areas and obtained correlation coefficients of 0.64 for Vogar, and 0.91 by combining faults from Vogar, Thingvellir and Sveinagja in northern Iceland.

World wide

MacMillan (1975) compiled a data set on the displacement and length of more than 125 continental strike-slip faults by conducting an extensive literature search (Fig. 1i). Unfortunately information on how the displacements were estimated was not documented. These data appear to be of very variable quality and some of these faults, such as the San Andreas fault in California, are not bounded faults. Inclusion of such data will result in spuriously high d/L values, since a transform fault can continue to accumulate displacement without the necessity of growing longer. Comparing MacMillan's data set to subsequent documentations of displacement on the same fault shows substantial disagreements. For example, MacMillan recorded an offset of 175 km for the North Anatolian Fault in Turkey, whereas Wesnousky (1988) references more recent work that estimates the offset on this fault to be between 25 and 45 km. Because this data set is for 100–1000 km long faults, and contains the highest d/L ratios of any recorded, many of these faults may be past or present plate boundaries. Ranalli (1977) presented a statistical analysis of MacMillan's data but, for the reasons listed above, we do not consider these statistical results to be meaningful. MacMillan's data set is potentially interesting but requires a detailed re-examination of the original sources, and the elimination of plate boundary faults before it may be used in a quantitative analysis.

Ocean basins

One data set from the ocean basins that has been included by some workers (e.g. Marrett & Allmendinger 1991) in the analysis of the fault scaling relationship, is the one compiled by Menard (1962). It is peculiar that Menard's data set has even been included in these discussions. His paper was published prior to the transform fault hypothesis (Wilson 1965), and most of his data set consists of the length of oceanic fracture zones plotted vs their ridge offsets.

Other quantitative studies of faults in the oceans are mostly concerned with normal faults that form at mid-ocean ridges. Estimates of average fault offset have been obtained from detailed bathymetric profiles which resolve offsets as small as a few meters across at the East Pacific Rise and the Mid-Atlantic Ridge (Lonsdale 1977, Lonsdale & Speiss 1977, MacDonald & Luyendyk 1977, Laughton & Searle 1979, Searle 1984, Bicknell *et al.* 1987, Kong *et al.* 1988). Average fault length has been estimated from sonar swath images which in some cases

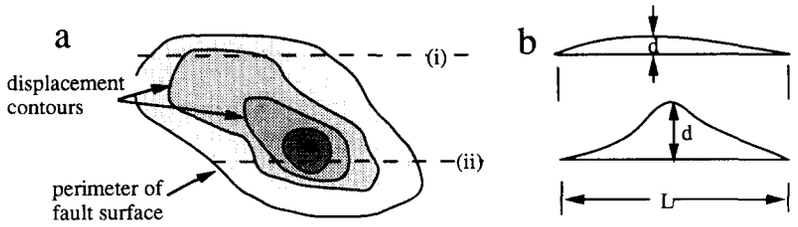

Fig. 2. Sketch showing (a) contoured displacement distributions on a fault surface: darker shades indicate larger displacements, the black dot indicates the maximum value of the displacement over the entire fault surface. (b) Two sampling lines (i) and (ii) across the fault surface shown in (a) (e.g. one near the surface and another at greater depth in the section) result in two different displacement profiles and different d/L ratios for the same fault.

resolve faults as short as a few hundred meters (Laughton & Searle 1979, Searle 1984, Carbotte & MacDonald 1990). However, problems are introduced by the resolution of the sonar imaging system, the registration of adjacent swaths, and the ambiguities of interpreting back-scatter information. Summaries of oceanic fault data have been compiled by Laughton & Searle (1979), Searle (1984) and Carbotte & MacDonald (1990).

Two other data sets

Marrett & Allmendinger (1991) also presented two other data sets, one is proprietary data from the Gulf of Mexico and the other data set is from Japan (Minor Faults Research Group 1973). The data from Japan were obtained from an annotated sketch map and three cross-section lines shown in that publication. Both datasets were untabulated and plot as broad scatter fields, so we have not attempted individual correlations, although we consider them with the collective data set (Fig. 3).

SOURCES OF SCATTER IN THE DATA

All the data sets shown in Fig. 1 are characterized by a significant amount of scatter, e.g. faults of similar length can have displacements that differ by a factor of 1.5–2.0. The reason for this can be attributed to both the geologic processes involved in faulting, and the methods by which the measurements are made.

The displacement distribution on a fault surface can often be quite irregular (e.g. see Rippon 1985) (Fig. 2). The maximum displacement may be unrepresentative or not related in a simple way to the average amount of displacement on the fault. For many of the published data sets only the maximum displacement is recorded. If the shape of a fault surface is also irregular, sampling the same fault at different structural levels (e.g. the level of exposure or locations of a mine plan) can affect the length estimates (see Walsh & Watterson 1987).

Muraoka & Kamata (1983) showed that contrasts in the mechanical properties of different lithologies can modify the shape of fault displacement profiles markedly for the meter-scale faults that they studied. Similar effects were observed by Peacock (1991), who found that fault growth was sometimes inhibited at the contact of dissimilar lithologic units.

Peacock & Sanderson (1991) showed that the displacement gradient towards the tip of a fault segment increases with the proximity of neighboring segments. This effect tends to produce asymmetry in the displacement profiles observed. As noted above, these workers found that the displacement/length ratios determined for the individual segments were systematically higher than that for the whole fault zone by about a factor of 2.

Walsh & Watterson (1987, 1988) found that displacement on the coalfield faults they studied is often distributed across more than one fault strand. Walsh & Watterson (1991) suggest that to obtain the correct displacement distribution for the composite structure it is necessary to add the displacements on the separate strands together. Another important effect documented by Walsh & Watterson (1987) from their observations of faulting in sedimentary rocks, is that a proportion of the total stratigraphic offset across a fault may be accommodated by drag folding of the adjacent strata.

An upper limit on the amount of displacement that can accumulate on normal faults is imposed by isostatic restoring forces. This is because of the topography generated in the foot-wall and hanging-wall blocks of the fault. This effect may destroy the correlation between d and L for large (tens of kilometers long) normal faults.

There may be differences in the ratio d/L if fault length is measured parallel vs perpendicular to the slip direction. For example, contoured displacement diagrams (e.g. Rippon 1985) show that normal faults in sedimentary strata are often elliptical in shape being longer in the strike direction by a factor of two or more in many cases. If this is the case, for a given maximum displacement on the fault plane the ratio d/L will vary depending on which dimension is considered.

DISCUSSION

Correlation for individual data sets

In addition to the scatter in the displacement–length data outlined above, there are several general problems with these data that make it difficult to establish a scaling relationship between d and L empirically. The first is that in any given region, the number of faults $N(L)$ with length $\geq L$, obeys a power-law relation of the form $N(L) = aL^{-C}$ (e.g. Scholz & Cowie 1990). Thus any data set will be dominated by the smaller faults with few of the largest faults, rendering a fit to the data statisti-

cally biased. This problem is evident in all of the data sets shown in Fig. 1. The second problem is that each data set spans only a limited size range of about one order of magnitude. This is too short a range to fit with an exponent in a log–log plot and requires the scatter to be much less than a factor of two or three to be fit reliably in a linear plot, a requirement not usually met by the data.

The data sets in Fig. 1 have been fit in two ways: the dashed line is given by $d = L^{1.5}/P$ (after Marrett & Allmendinger 1991), and the solid line is a linear fit constrained to go through the origin. A value of P was estimated for each data set by plotting the data on log–log axes and determining the intercept (i.e. log P) (see Table 1, the value $P = 200$ is from the Marrett & Allmendinger 1991 regression). Visual inspection of Fig. 1 shows that the non-linear fit tends to over-predict the displacement for the larger faults. Each data set is consistent with the linear fit but with a different constant of proportionality (equal to the slope), γ, in each case (Table 1). The linear fits, however, are poorly constrained. Because the data are power-law distributed, not Gaussian, standard linear regression methods to obtain a correlation coefficient are not permitted. Instead, the variance in the data is measured about the two curve fits and in Table 1 we have shown the percentage increase or reduction in the variance if the non-linear fit is used rather than the linear fit. In seven out of the nine data sets plotted, the variance increases substantially if the higher-order function is used. Even for the two cases where the variance is reduced with the use of the non-linear function we argue, by Ockham's Razor, that the data do not demand fitting by a higher-order function given that the number of degrees of freedom is increased in that case.

Correlation for the combined data set

Since the data sets of Fig. 1, taken together, cover a wide range of length scales, one way to improve the confidence in a regression is to combine them. Thus in Fig. 3, all the data are plotted in log–log co-ordinates. The dataset of MacMillan (1975) are included for completeness, even though we consider it least reliable. Also shown are the three published interpretations, based on different subsets of the data.

Watterson (1986) and Walsh & Watterson (1988) interpretated the data as lying on a family of lines of slope equal to 2 according to equation (1), where

$$P = 8a\left[\frac{\Lambda\mu}{\Delta\sigma}\right]^2, \tag{3}$$

where $\Delta\sigma$ is the stress drop of individual earthquakes on the fault, Λ is a geometrical constant, and a is a constant which specifies the increase in the increment of slip during successive earthquakes. Walsh & Watterson (1988) argue that different data sets lie along lines of different P (e.g. Table 1), which they ascribe to variations in the shear modulus, μ. Thus they explained Muraoka & Kamata's (1983) data by assuming a lower shear modulus for those data.

On the other hand, Marrett & Allmendinger (1991) fit a single line through all their data. The implication of their interpretation is that there is a 'universal' scaling law for faults, independent of the material properties (i.e. P is a universal constant in this case). Our interpretation, based on the individual data sets rather than a combined one and argued through the model described by equation (2), is that each data set has a linear relationship between d and L; different constants of proportionality reflect variations in the material properties σ_0 and μ.

The Marrett & Allmendinger (1991) regression line fits the data for faults with lengths greater than about 300 m, but not the smaller faults. However, if the displacement–length scaling relationship does depend on material properties then this type of fit is not valid unless one can argue independently that these properties are the same for all the data sets that are fit. If a physical model predicts the correct slope, one can argue this case more persuasively. The model proposed by Watterson (1986) and Walsh & Watterson (1988) was clearly motivated by the interpretation that the data indicated a quadratic growth law. The central assumption in their model is that each successive slip event on the fault is larger by a constant increment than the preceding one. No physical basis for this assumption is given: its main feature is that it results in a quadratic displacement–length relationship. Further, it is noted that Marrett & Allmendinger (1991) subsequently altered the central assumption of this model to make it consistent with an exponent of 1.5. As Walsh & Watterson (1988) admit "the arithmetic growth model incor-

Table 1. Increase (+) or decrease (−) in variance if non-linear fit to the data is used instead of linear fit

	P	γ	Variance reduction (−)/increase (+)
Elliott (1976)	200	6×10^{-2}	−60%
Krantz (1988)	200	7×10^{-3}	51%
Walsh & Watterson (1987)	200	6×10^{-3}	99%
Peacock & Sanderson (1991)	20	9×10^{-3}	74%
Peacock (1991)	3	1.5×10^{-2}	241%
Villemin *et al.* (in press)	100	2.9×10^{-2}	422%
Muraoka & Kamata (1983)	4	1.2×10^{-2}	−37%
Opheim & Gudmundsson (1989)	100	1.2×10^{-3}	647%
MacMillan (1975)	200	1.7×10^{-1}	23%

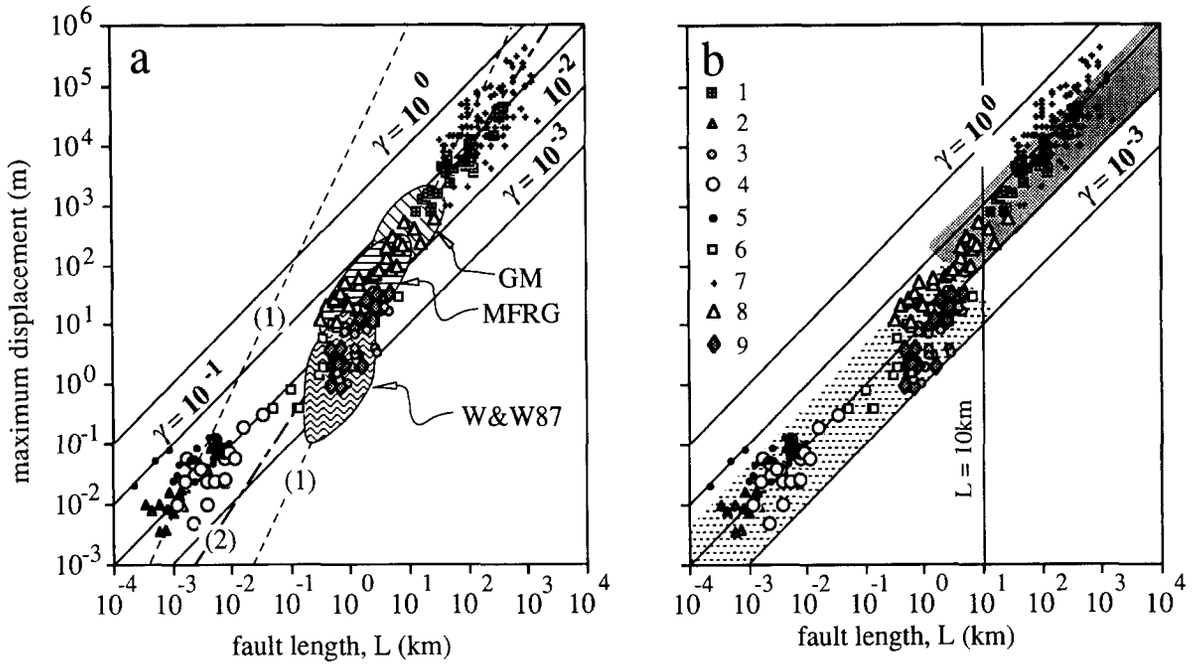

Fig. 3. Log–log plots of maximum displacement and length data shown in Fig. 1. 1, Elliott (1976); 2, Muraoka & Kamata (1983); 3, Walsh & Watterson (1987); 4, Peacock & Sanderson (1991); 5, Peacock (1991); 6, Opheim & Gudmundsson (1989); 7, MacMillan (1975); 8, Villemin *et al.* (in press); 9, Krantz (1988). Shaded ellipses indicate other data sets compiled by Walsh & Watterson (1987), Marrett & Allmendinger (1991) from Gulf of Mexico (GM) and the work of the Minor Faults Research Group (1973) (MFRG). Solid lines are lines of constant ratio d/L denoted by γ values. (a) Dashed lines indicate correlations proposed by (1) Watterson (1986) and Walsh & Watterson (1988) and (2) Marrett & Allmendinger (1991); (b) shaded areas indicate the difference between small ($L \leq 10$ km), upper crustal faults ($10^{-3} \leq \gamma \leq 3 \times 10^{-2}$) and large faults ($L \geq 10$ km) that penetrate through the crust ($3 \times 10^{-2} \leq \gamma \leq 2 \times 10^{-1}$).

porates no explanation for fault growth". Thus this 'model' is no more than an interpretation of the data and cannot be used to justify, or further embellish, that interpretation.

The parameter γ, which is the ratio of displacement to fault length (d/L) can be recognized as a critical shear strain for fault propagation. In the particular model we introduced (Cowie & Scholz 1992b), this ratio determines the magnitude of the finite stress concentration at the ends of the faults which, for an actively growing fault, must be just equal to the shear strength of the surrounding rock, σ_o. If a fault is growing in a rock with constant σ_o then d/L must be constant (represented by solid lines with slope of 45° in Fig. 3). A non-linear relationship between d and L implies that σ_o varies systematically with fault size, for which we find no physical basis. On the other hand, since γ is the ratio of two material properties (equation 2), it should be expected to vary between data sets. For this reason we maintain that each data set should be analysed separately and that combining data sets together is incorrect.

Our summary interpretation of all the data sets is shown in Fig. 3(b). Faults with lengths of 1 km or more appear to have systematically higher values of γ than shorter faults. We suggest therefore that there may be a cross-over phenomenon between 'large' faults that cut through the entire thickness of the brittle upper crust ($L \geq 10$ km) and 'small' faults that do not. This cross-over could be because large faults are two-dimensional, being only constrained at their ends, whereas small faults are three-dimensional and are pinned along their entire perimeter. Another explanation is simply that large faults rupture stronger rock on average. Such a cross-over phenomena is observed for earthquakes (Shimazaki 1986). On the other hand, in the mid-scale range where most of the data has been collected, the faults exhibit a wide range of γ values, and this may turn out to be the case also in the small- and large-scale range as more data are collected there.

Finally, it must be stated that none of these data are really conclusive, otherwise it would not be possible for such a wide divergence of opinion to exist. What is needed are data that span a much greater scale range for faults in a single tectonic environment and rock type. It is more likely that such data will be found in the smaller, rather than the larger scale, range.

Acknowledgements—The authors wish to thank David Peacock for providing access to his data and Thiery Villemin for providing a preprint of his paper. Steve Wojtal provided a copy of an unpublished manuscript by David Elliott. Critical reviews by Agust Gudmundsson, John Walsh and David Peacock helped to improve considerably the final manuscript. This work was supported by NFS contract No. EAR90-04534. Lamont contribution No. 4913.

REFERENCES

Anderson, E. M. 1942. *The Dynamics of Faulting* (1st edn). Oliver & Boyd, Edinburgh.

Bicknell, J. D., Sempere, J.-C. & MacDonald, K. C. 1987. Tectonics

of a fast spreading center: A Deep-Tow and Sea Beam survey of the East Pacific Rise at 19°30'S. *Marine geophys. Res.* **9**, 25–45.
Boyer, S. E. & Elliott, D. 1982. Thrust systems. *Bull. Am. Ass. Petrol. Geol.* **66**, 1196–1230.
Carbotte, S. M. & MacDonald, K. C. 1990. Causes of variation in fault facing direction in the ocean floor. *Geology* **18**, 749–752.
Cowie, P. A. & Scholz, C. H. 1992a. Growth of faults by accumulation of seismic slip. *J. geophys. Res.* **97**, 11,085–11,096.
Cowie, P. A. & Scholz, C. H. 1992b. Physical explanation for the displacement–length relationship for faults using a post-yield fracture mechanics model. *J. Struct. Geol.* **14**, 1133–1148.
Elliott, D. 1976. The energy balance and deformation mechanisms of thrust sheets. *Phil. Trans. R. Soc. Lond.* **A283**, 289–312.
Gibbs, D. A. 1984. Structural evolution of extensional basin margins. *J. geol. Soc. Lond.* **141**, 609–620.
Gibson, J. R., Walsh, J. J. & Watterson, J. 1989. Modelling of bed contours and cross-sections adjacent to planar normal faults. *J. Struct. Geol.* **11**, 317–328.
Gudmundsson, A. 1987a. Geometry, formation and development of tectonic fractures on the Reykjanes Peninsula, Southwest Iceland. *Tectonophysics* **139**, 295–308.
Gudmundsson, A. 1987b. Tectonics of the Thingvellir fissure swarm, SW Iceland. *J. Struct. Geol.* **9**, 61–69.
Gudmundsson, A. In press. Formation and growth of normal faults at the divergent plate boundary in Iceland. *Terra Nova* **4**.
Kong, S. L., Detrick, R. S., Fox, P. J., Maya, L. F. & Ryan, W. B. F. 1988. Morphology and tectonics of the Mark area from Sea Beam and Sea MARC observations (Mid-Atlantic Ridge 23°N). *Marine geophys. Res.* **10**, 59–90.
Krantz, R. W. 1988. Multiple fault sets and three-dimensional strain: theory and application. *J. Struct. Geol.* **10**, 225–237.
Laughton, A. S. & Searle, R. C. 1979. Tectonic processes on slow spreading ridges. In: *Deep Drilling Results in the Atlantic Ocean: Ocean Crust* (edited by Talwani, M., Harrison, C. G. & Hayes, D. E.). *Am. Geophys. Un. Geophys. Monogr.* **2**, 15–32.
Lonsdale, P. 1977. Structural geomorphology of a fast spreading rise crest: The East Pacific Rise near 3°S. *Marine geophys. Res.* **3**, 251–293.
Lonsdale, P. & Spiess, F. N. 1977. Deep-tow observations at the East Pacific Rise, 8°45'N, and some interpretations. *Init. Rep. Deep Sea Drilling Proj.* **54**, 43–62.
MacDonald, K. C. & Luyendyk, B. P. 1977. Deep tow studies of the structure of the mid-Atlantic Ridge crest near lat 37°N. *Bull. geol. Soc. Am.* **88**, 621–636.
MacMillan, R. A. 1975. The orientation and sense of displacement of strike-slip faults in continental crust. Unpublished B.Sc. thesis, Carlton University, Ottawaa, Ontario.
Marrett, R. & Allmendinger, R. W. 1991. Estimates of strain due to brittle faulting: sampling of fault populations. *J. Struct. Geol.* **13**, 735–7737.
Menard, H. W. 1962. Correlation between length and offset on very large wrench faults. *J. geophys. Res.* **67**. 4096–4098.
Minor Faults Research Group. 1973. A minor fault system around the Otaki Area, Boso Peninsula, Japan. *Chiky-u Kagaku (Tokyo, Japan)* **27**, 180–187.
Muraoka, H. & Kamata, H. 1983. Displacement distribution along minor fault traces. *J. Struct. Geol.* **5**, 483–495.
Opheim, J. A. & Gudmundsson, A. 1989. Formation and geometry of fractures, and related volcanism, of the Krafla fissure swarm, northeast Iceland. *Bull. geol. Soc. Am.* **101**, 1608–1622.
Peacock, D. C. P. 1991. Displacement and segment linkage in strike-slip fault zones. *J. Struct. Geol.* **13**, 1025–1035.
Peacock, D. C. P. & Sanderson, D. J. 1991. Displacement and segment linkage and relay ramps in normal fault zones. *J. Struct. Geol.* **13**, 721–733.
Ranalli, G. 1977. Correlation between length and offset on strike-slip faults. *Tectonophysics* **37**, 1–7.
Rippon, J. H. 1985. Contoured patterns of the throw and hade of normal faults in the Coal Measures (Westphalian) of northwest Derbyshire. *Proc. Yorks. geol. Soc.* **45**, 147–161.
Schlische, R. 1991. Half-graben basin filling models: new constraints on continental basin development. *Basin Res.* **3**, 123–141.
Scholz, C. H. & Cowie, P. A. 1990. Determination of geologic strain from fault slip data. *Nature* **346**, 837–839.
Searle, R. 1984. GLORIA survey of the East Pacific Rise near 3.5°S: Tectonic and volcanic characteristics of a fast-spreading mid-ocean ridge. *Tectonophysics* **101**, 319–344.
Shimazaki, K. 1986. Small and large earthquakes: The effects of the thickness of the seismogenic layer and the free surface. In: *Earthquake Source Mechanics* (edited by Das, S., Boatwright, J. & Scholz, C.). *Am. Geophys. Un. Geophys. Monogr.* **37**, 209–219.
Villemin, T., Angelier, J. & Sunwoo, C. In press. Fractal distribution of fault length and offset: Implications on brittle deformation evaluation: The Lorraine Coal Basin (NE France). In: *Fractals and Their Use in the Petroleum Industry* (edited by Barton, C. & LaPointe, P.). Am. Ass. Petrol. Geol. Book Series.
Villemin, T. & Sunwoo, C. 1987. Distribution logarithmique self-similaire des rejets et longuers de failles: Examples du Bassin Houiller, Lorraine. *C. r. Acad. Sci., Paris* **305**, 1309–1312.
Watterson, J. 1986. Fault dimensions, displacements and growth. *Pure & Appl. Geophys.* **124**, 365–373.
Walsh, J. J. & Watterson, J. 1987. Distribution of cumulative displacement and of seismic slip on a single normal fault surface. *J. Struct. Geol.* **9**, 1039–1046.
Walsh, J. J. & Watterson, J. 1988. Analysis of the relationship between displacements and dimensions of faults. *J. Struct. Geol.* **10**, 239–247.
Walsh, J. J. & Watterson, J. 1991. Geometric and kinematic coherence and scale effects in normal fault systems. In: *Geometry of Normal Faults. Spec. Publs geol. Soc. Lond.* **56**, 193–206.
Wernicke, B. & Burchfiel, B. C. 1982. Modes of extensional tectonics. *J. Struct. Geol.* **4**, 105–115.
Wesnousky, S. G. 1988. Seismological and structural evolution of strike-slip faults. *Nature* **335**, 340–342.
Wilson, T. 1965. A new class of faults and their bearing on continental drift. *Nature* **270**, 343.